analytical chemistry

pubs.acs.org/ac Article

Probing N-Heterocyclic Carbene Surfaces with Laser Desorption Ionization Mass Spectrometry

Nathaniel L. Dominique, Shelby L. Strausser, Jacob E. Olson, William C. Boggess, David M. Jenkins,* and Jon P. Camden*

Cite This: *Anal. Chem.* 2021, 93, 13534−13538 Read Online

ACCESS | Metrics & More | Article Recommendations | Supporting Information

ABSTRACT: The proliferation of N-heterocyclic carbene (NHC) self-assembled monolayers (SAMs) on gold surfaces stems from their exceptional stability compared to conventional thiol-SAMs. The prospect of biological applications for NHC-SAMs on gold shows the need for biocompatible techniques (e.g., large biomolecule detection and high throughput) that assesses SAM molecular composition. Herein, we demonstrate that laser desorption ionization mass spectrometry (LDI-MS) is a powerful and facile probe of NHC surface chemistry. LDI-MS of prototypical imidazole-NHC- and benzimidazole-NHC-functionalized AuNPs yields exclusively $[NHC_2Au]^+$ ions and not larger gold clusters. Employing benzimidazole-NHC isotopologues, we explore how monolayers pack on a single AuNP and the lability of the NHCs once ligated. Quantitative analysis of the homoleptic and heteroleptic $[NHC_2Au]^+$ ions is performed by comparing to a binomial model representative of a randomized monolayer. Lastly, the reduction of nitro-NHC-AuNPs to amine-NHC-AuNPs is tracked via LDI-MS signals, illustrating the ability of LDI-MS to probe postsynthetic modifications of the anchored NHCs, which is critical for current and future applications of NHC surfaces.

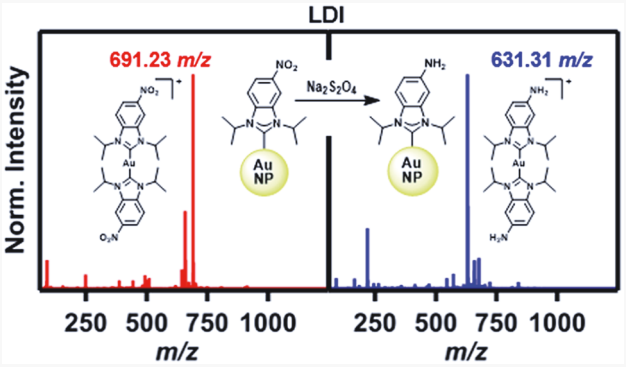

N-heterocyclic carbene (NHC) ligands' strong metal-carbon bonds and highly tunable structures enable numerous applications, including organometallic catalysis,[1−3] electronics,[4] supramolecular chemistry,[5] metal−organic frameworks,[6] and medicinal chemistry.[7] To add to this considerable collection, NHCs were recently shown to form robust self-assembled monolayers (SAMs)[8−10] stable under electrochemical cycling,[11] high temperatures,[12−14] catalytic cycling,[15,16] and exposure to rigorous chemical environments,[17−20] signifying that they are an attractive alternative to the widely used, but labile, thiols in noble-metal surface functionalization.[21] The longevity of implantable electrochemical sensors, for example, is currently limited by the instability of thiol-SAMs.[22]

Although numerous methods are available for probing the molecular and structural characteristics of NHC-SAMs, relatively few methods are high-throughput and easily applied to biocompatible NHC-SAMs (Figure 1). Scanning tunneling microscopy (STM) elucidates NHC ligand packing[11] and movement,[23] whereas atomic force microscopy paired with infrared spectroscopy (AFM-IR) provides spectroscopic evidence of chemical reactions on the surface.[24] Elucidation of NHC chemisorption often relies on X-ray photoelectron spectroscopy (XPS),[25,26] although it is difficult to distinguish similar chemical structures using XPS. Characterization of the local ligand composition of monolayers frequently relies on time-of-flight secondary-ion mass spectrometry (ToF-SIMS).[27] Although STM, AFM-IR, XPS, and ToF-SIMS are powerful probes of fundamental carbene surface chemistry, their compatibility with complex systems, throughput, and accessibility remains limited.

Other characterization methods provide versatile and biocompatible probes of NHC monolayers but are restricted to specific analytes and matrices. For instance, surface-enhanced Raman spectroscopy (SERS) provides surface-sensitive characterization of NHC ligands[28] but only probes species very near to the surface.[29] Nuclear magnetic resonance (NMR) spectroscopy delivers molecular structure information[30] but is hindered in complex media by spectral convolution. Limitations across the most common current techniques and the prospect of NHC-SAM biological applications illustrate the need for a high-throughput, biocompatible technique capable of characterizing the molecular composition of NHC monolayers.

Received: June 7, 2021
Accepted: September 13, 2021
Published: September 28, 2021

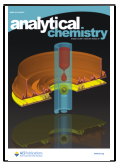

https://doi.org/10.1021/acs.analchem.1c02401
Anal. Chem. 2021, 93, 13534−13538

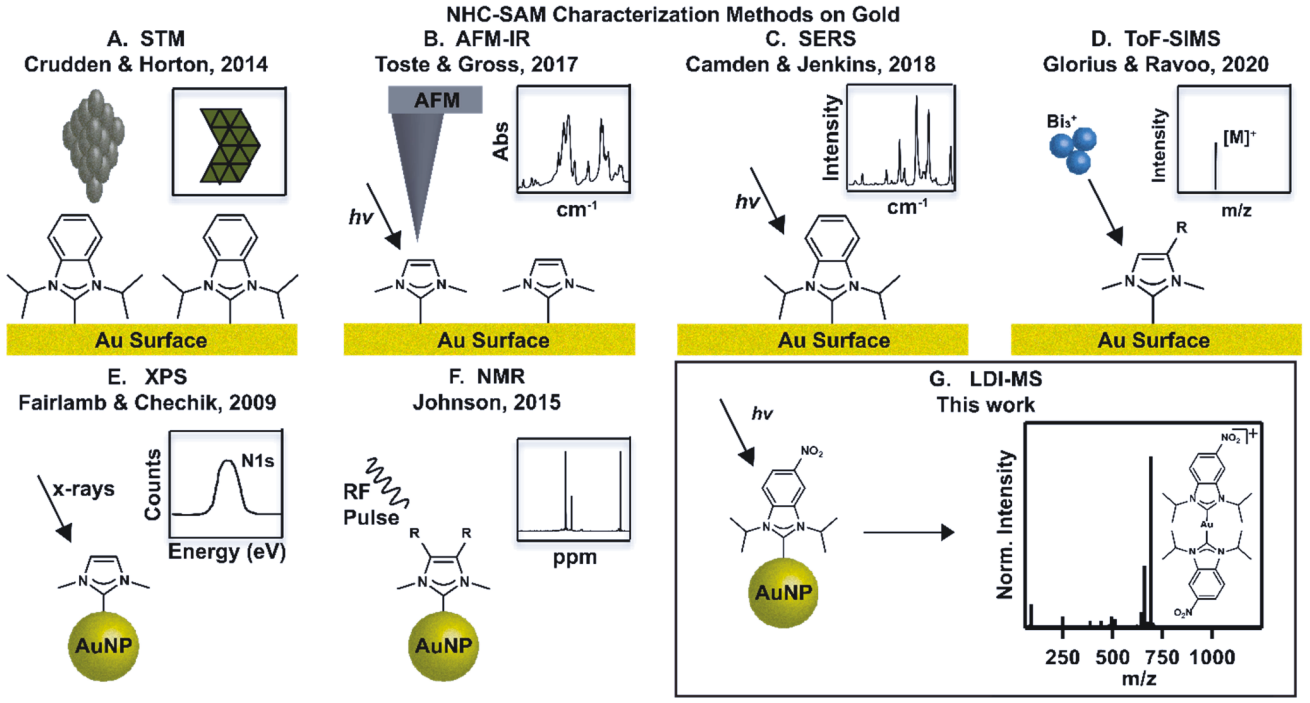

Figure 1. Selected NHC-SAM characterization methods on gold surfaces (A–D) or nanoparticles (E, F). LDI-MS characterization provides a facile and accessible method for probing postsynthetic modifications of the NHC surface on nanoparticles (G).

Laser desorption ionization mass spectrometry (LDI-MS) is a well-established method for the characterization of SAMs on nanomaterials[31,32] and surfaces.[33] This technique enables high-throughput screening of chemical reactions[34] and large biomolecules on SAMs.[35] Compared to ToF-SIMS, LDI-MS offers routine detection of analytes beyond 10,000 m/z,[36] high throughput, and complementary desorption and ionization methods (i.e., laser-induced processes).[37] Finally, monolayers with strong metal–ligand bonds and dense surface packing provide high signal-to-noise ratios,[38] which is ideal because NHC-SAMs on Au surfaces display these characteristics.[39] Therefore, we hypothesized that LDI-MS will be especially suitable for NHC-modified surfaces and for investigating their chemical reactions. Despite its promise, to date, only two reports tangentially employ LDI-MS to study NHC-SAMs.[40,41]

In this study, we demonstrate the power and versatility of LDI-MS for probing the chemical composition and transformations of NHC-functionalized gold nanoparticles. We establish a basic understanding of the desorption and ionization characteristics of NHC surfaces by first measuring the prototypical imidazole-NHC- and benzimidazole-NHC-functionalized AuNPs. We investigate how these spectra encode information about the local monolayer structure using benzimidazole-NHC isotopologues. These isotopic mixtures of NHCs also provide evidence on NHC transfer between AuNPs. Finally, we employ LDI-MS to monitor chemical transformations of the surface-bound NHCs, specifically the reduction of a nitro to an amine on the 4-position of the benzimidazole-NHC ring.

EXPERIMENTAL SECTION

Figure 2 illustrates the structure of the carbene ligands and carbene-functionalized gold nanoparticles (NHC-AuNPs) interrogated in this study. Complexes $[(\mathbf{1})_2\mathrm{Au}]\mathrm{Cl}$, (**2**)AuCl, and $[(\mathbf{4})_2\mathrm{Au}]\mathrm{I}$ were previously reported.[42−44] Details of the

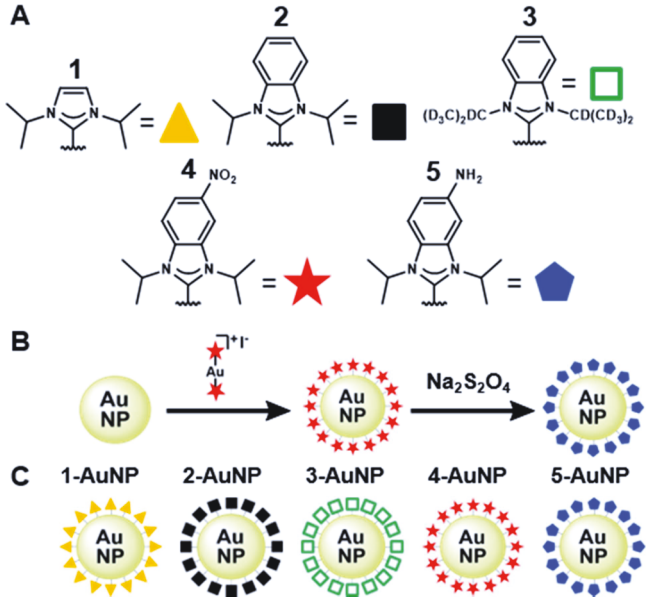

Figure 2. (A) NHC structures shown with representative shapes and numerical identifiers; (B) schematic illustrates AuNP functionalization with carbenes and the reduction of **4-AuNP** to form **5-AuNPs**; (C) carbene AuNPs shown with representative shapes and identifiers.

synthesis and characterization of (**3**)AuCl are given in the Supporting Information. NHC-AuNPs were prepared according to our previously described procedure.[44] Briefly, $[(\mathbf{1})_2\mathrm{Au}]\mathrm{Cl}$, (**2**)AuCl, (**3**)AuCl, and $[(\mathbf{4})_2\mathrm{Au}]\mathrm{I}$ were dissolved in acetonitrile and added to aqueous citrate-capped AuNPs to generate a solution with a final ligand concentration of 0.72, 1, 1, and 0.59 μM, respectively (Figure 2B). The resulting solution was mixed vigorously under ambient conditions for 15 min. The mixed carbene monolayers were prepared by adding an aliquot of premixed (**2**)AuCl and (**3**)AuCl stock solutions

https://doi.org/10.1021/acs.analchem.1c02401
Anal. Chem. 2021, 93, 13534−13538

to AuNPs according to the aforementioned procedure. The synthesis of **5-AuNPs** was performed by adding 5 mL of **4-AuNPs** to ~1 mg of sodium dithionite.[44] The suspension of **5-AuNPs** was then mixed for 15 min under ambient conditions.

To remove the background LDI signal arising from the residual citrate[45] and ions (e.g., sodium chloride),[46] several washing steps were used. The functionalized nanoparticles were centrifuged at 10,000 rpm for 20 min, and the supernatant was removed with a pipette. This process was repeated before each resuspension in ultrapure water (18 MΩ), reagent alcohol, and lastly a 1:1 mixture of reagent alcohol to ultrapure water. After washing, two successive 1.5 μL aliquots of the sonicated suspension were drop-cast onto an LDI-MS target plate and dried in air. This process was repeated for all LDI-MS samples of NHC-AuNPs. Mixed nanoparticles were prepared by adding 100 μL of prewashed **2-AuNPs** and 100 μL of prewashed **3-AuNPs** with 15 min of vigorous shaking. MS analysis of NHC-AuNPs was performed on a Bruker UltrafleXtreme MALDI TOF-TOF mass spectrometer equipped with a 355 nm laser.

RESULTS AND DISCUSSION

Our LDI-MS investigation of AuNPs functionalized with NHCs began by comparing the ions formed from the two most studied NHCs. LDI-MS of **1-AuNPs** and **2-AuNPs** generates $[(\mathbf{1})_2\mathrm{Au}]^+$ and $[(\mathbf{2})_2\mathrm{Au}]^+$ ions, respectively (Figure 3).

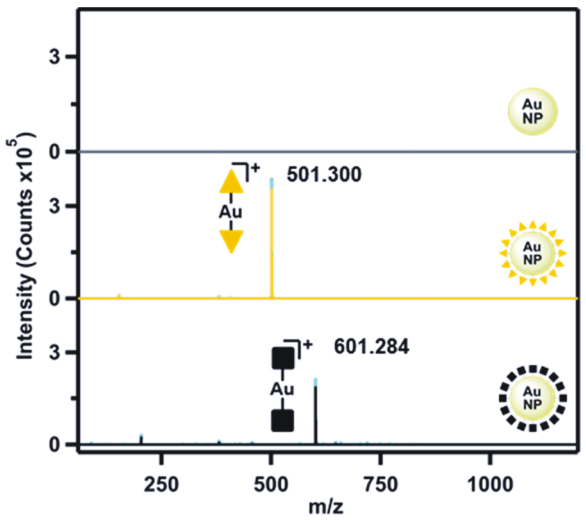

Figure 3. Collection of LDI-MS spectra for **AuNPs** (top), **1-AuNPs** (middle), and **2-AuNPs** (bottom) demonstrates the formation of $[\mathrm{NHC_2Au}]^+$ ions for **1-AuNPs** and **2-AuNPs**. Teal lines illustrate 95% confidence intervals from >12 spectra.

Notably, no higher mass gold clusters are observed. These ions form readily without any organic matrix to facilitate desorption and ionization. Avoiding the addition of an organic matrix generates an optimal system for LDI-MS analysis below 500 m/z by minimizing spectral convolution.[46] As a control experiment, stock solutions of the starting materials $[(\mathbf{1})_2\mathrm{Au}]$Cl and (**2**)AuCl were deposited, and after drying, LDI was performed. Despite the greatly increased concentrations in the control experiments, the control signal is more than two orders of magnitude weaker than the signal observed from **1-AuNPs** and **2-AuNPs**. This result illustrates that the ions shown in Figure 3 are attributed to a desorption process mediated by the nanoparticles (Figures S7 and S8).

To understand the packing and potential scrambling of NHCs in the SAM on AuNPs, we conducted a set of ligand-mixing experiments. A deuterated analog of (**2**)AuCl was synthesized: (**3**)AuCl (Figure 2A, see the Supporting Information for details). Figure 4 presents spectra of NHC-

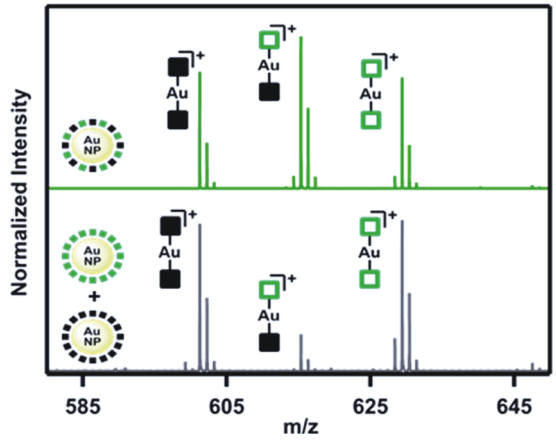

Figure 4. LDI-MS spectra of mixed monolayer **AuNPs** (top) compared with spectra obtained from mixing **2-AuNPs** and **3-AuNPs** for 15 min after functionalization (bottom). The preferential formation of heteroleptic ions occurs only in the mixed monolayer sample.

functionalized AuNPs obtained from two different experiments. In the top panel, solutions of (**2**)AuCl and (**3**)AuCl were mixed in a 1:1 ratio before addition to the AuNPs, while in the bottom panel, **2-AuNP** and **3-AuNP** were mixed together for a total of 15 min after functionalization. The mixed monolayer AuNPs (top) preferentially form heteroleptic $[(\mathbf{2})(\mathbf{3})\mathrm{Au}]^+$ ions at 615.341 m/z, whereas the mixture of **2-AuNPs** and **3-AuNPs** preferentially form homoleptic $[(\mathbf{2})_2\mathrm{Au}]^+$ and $[(\mathbf{3})_2\mathrm{Au}]^+$ ions at 601.217 m/z and 629.432 m/z, respectively (bottom).

These combined data illustrate that the ion observed depends on the neighboring ligands in the monolayer. If plume chemistry was responsible for heteroleptic ion formation, the relative signal intensity of $[(\mathbf{2})(\mathbf{3})\mathrm{Au}]^+$ ions in spectra corresponding to the **2-AuNPs** and **3-AuNPs** mixture would resemble that of mixed monolayer AuNPs. Because the formation of heteroleptic ions relates to the proximity of carbenes on the surface, this result proves that LDI-MS analysis provides a window into the local surface structure of the NHC monolayers prior to desorption and ionization.

The observed signal ratios of the $[(\mathbf{2})_2\mathrm{Au}]^+$, $[(\mathbf{2})(\mathbf{3})\mathrm{Au}]^+$, and $[(\mathbf{3})_2\mathrm{Au}]^+$ ions are in quantitative agreement with a binomial model that assumes a random distribution of the NHC ligands. Employing a sum-of-square residuals (SSR) calculation can illustrate deviations of the experimental data from the binomial model and SSR values less than 10^{-2} are characteristic of well-mixed monolayers.[47] We obtain SSR values of 4.7×10^{-3} for the mixed monolayers and 0.2 for the mixed **2-AuNPs** and **3-AuNPs** samples; therefore, a signal distribution characteristic of well-mixed SAMs is present only in the spectra of the mixed monolayers (Figure 4, top) not **2-AuNPs** mixed with **3-AuNPs** (Figure 4, bottom). We confirmed this result by preparing mixed monolayers with different concentration ratios of (**2**)AuCl and (**3**)AuCl (Figure S9) and report SSR values that are $<10^{-3}$ for all spectra (Table S5). This quantitative comparison provides additional evidence

https://doi.org/10.1021/acs.analchem.1c02401
Anal. Chem. 2021, 93, 13534−13538

of the local surface structure information contained in the observed ions.

LDI-MS is a powerful probe for observing chemical modifications of surfaces,[48] and the strong NHC signal observed here (Figure 3) suggested the potential for reaction monitoring of NHC-SAMs. To test this hypothesis, we reduced a nitro on the backbone of the NHC to an amine with sodium dithionite (Figure 2B) via a previously reported procedure.[44] Aqueous **4-AuNPs** were reacted with a slight excess of a reductant, yielding **5-AuNPs**. The spectra of **4-AuNPs** have a characteristic signal at 691.287 m/z corresponding to $[(\mathbf{4})_2\mathrm{Au}]^+$ ions (Figure 5, top). After

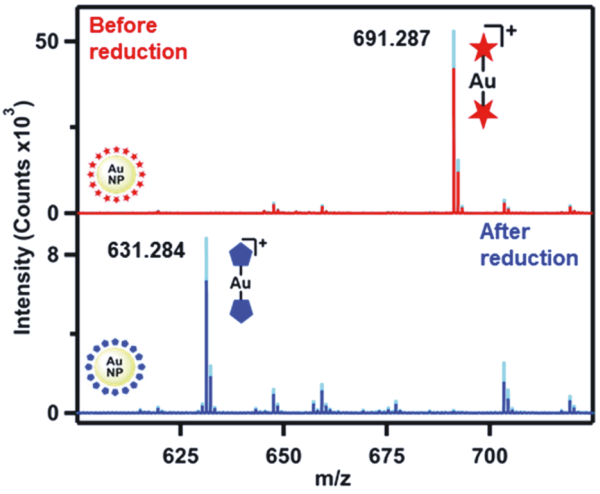

Figure 5. LDI-MS spectra of **4-AuNPs** before reduction (top) and **5-AuNPs** after reduction (bottom). The disappearance of $[(\mathbf{4})_2\mathrm{Au}]^+$ and the appearance of $[(\mathbf{5})_2\mathrm{Au}]^+$ after the reduction of **4-AuNPs** demonstrate the ability to track NHC surface reactions with LDI-MS. Teal lines illustrate 95% confidence intervals from 18 spectra.

reduction, the spectra are dominated by a signal at 631.284m/z corresponding to $[(\mathbf{5})_2\mathrm{Au}]^+$ ions, indicating the formation of **5-AuNPs** (Figure 5, bottom). Analysis of the $[(\mathbf{4})_2\mathrm{Au}]^+$, $[(\mathbf{4})(\mathbf{5})\mathrm{Au}]^+$, and $[(\mathbf{5})_2\mathrm{Au}]^+$ signals reveals that amine-NHC ligands compose >90% of the total peak area (Table S7). Furthermore, we demonstrate the capability of LDI-MS to track additional postsynthetic modifications by performing an amide linkage between benzoic acid and **5-AuNPs**. The data, illustrated graphically in Figure S11, demonstrate simultaneous detection of benzoic acid-modified amine-NHC ligands and unmodified amine-NHC ligands. Therefore, LDI-MS provides a detailed picture of the carbene monolayer composition, following chemical reactions on the surface.

CONCLUSIONS

We have demonstrated that LDI-MS is a powerful and facile method to probe the local structure and track chemical changes of NHC-SAMs on AuNPs. Classic imidazole- and benzimidazole-NHCs only yield single ions, not clusters, which makes tracking the NHCs on the surface straightforward. NHC isotopologues allow us to probe the local structure of the NHC monolayers, and, notably, LDI-MS measurements show that NHCs do not traverse between AuNPs once bound to a surface. More generally, this approach is found to be a facile and effective method for tracking chemical transformations of the surface-bound NHCs. These combined attributes, along with ease of application, indicate that LDI-MS is a highly effective tool for monitoring NHCs on surfaces. Given the ever-increasing expansion of NHC surface chemistries,[49,50] we expect LDI-MS to find significant applications across a wide variety of functionalized nanoparticles and planar surfaces.[51]

ASSOCIATED CONTENT

Supporting Information

The Supporting Information is available free of charge at https://pubs.acs.org/doi/10.1021/acs.analchem.1c02401.

Synthesis and characterization of carbene gold(I) complexes, detailed experimental methods, and additional data. (PDF)

AUTHOR INFORMATION

Corresponding Authors

David M. Jenkins − *Department of Chemistry, University of Tennessee, Knoxville, Knoxville, Tennessee 37996, United States;* orcid.org/0000-0003-2683-9157; Email: jenkins@ion.chem.utk.edu

Jon P. Camden − *Department of Chemistry and Biochemistry, University of Notre Dame, Notre Dame, Indiana 46556, United States;* orcid.org/0000-0002-6179-2692; Email: jon.camden@nd.edu

Authors

Nathaniel L. Dominique − *Department of Chemistry and Biochemistry, University of Notre Dame, Notre Dame, Indiana 46556, United States;* orcid.org/0000-0002-0439-9982

Shelby L. Strausser − *Department of Chemistry, University of Tennessee, Knoxville, Knoxville, Tennessee 37996, United States*

Jacob E. Olson − *Department of Chemistry and Biochemistry, University of Notre Dame, Notre Dame, Indiana 46556, United States;* orcid.org/0000-0001-7110-1739

William C. Boggess − *Department of Chemistry and Biochemistry, University of Notre Dame, Notre Dame, Indiana 46556, United States*

Complete contact information is available at: https://pubs.acs.org/10.1021/acs.analchem.1c02401

Author Contributions

All authors have given approval to the final version of the manuscript.

Notes

The authors declare no competing financial interest.

ACKNOWLEDGMENTS

This work is supported by the National Science Foundation under grant numbers CHE-1709566 (J.E.O. and J.P.C.), CHE-2108330 (N.L.D. and J.P.C.), CHE-1709468 (S.L.S. and D.M.J.), and CHE-2108328 (D.M.J.). Any opinions, findings, and conclusions or recommendations expressed in this material are those of the authors and do not necessarily reflect the views of the National Science Foundation. The authors thank Matthew Champion for constructive conversations regarding LDI-MS, Joseph DeJesus and Rowan Borsari for their work in synthesizing gold(I) carbene complexes, the Mass Spectrometry and Proteomics Facility at the University of Notre Dame for use of the Bruker UltrafleXtreme instrument, and Alexander Mukasyan and Tatyana Orlova for their assistance with SEM

imaging through the Notre Dame Electron Microscopy Facility.

■ ABBREVIATIONS

LDI-MS	laser desorption ionization mass spectrometry
NHC	N-heterocyclic carbene
SAM	self-assembled monolayer
AuNP	Au nanoparticle

■ REFERENCES

(1) Marion, N. Chapter 11:NHC−Copper, Silver and Gold Complexes in Catalysis. In *N-Heterocyclic Carbenes: From Laboratory Curiosities to Efficient Synthetic Tools*; Diez-Gonzalez, S., Ed.; Royal Society of Chemistry: Cambridge, England, 2010, 317−344. DOI: 10.1039/9781849732161-00317.

(2) Vougioukalakis, G. C.; Grubbs, R. H. *Chem. Rev.* **2010**, *110*, 1746−1787.

(3) Jenkins, D. M. *Synlett* **2012**, *23*, 1267−1270.

(4) Kang, S.; Byeon, S. E.; Yoon, H. J. *Bull. Korean Chem. Soc.* **2021**, *42*, 712−723.

(5) Sinha, N.; Hahn, F. E. *Acc. Chem. Res.* **2017**, *50*, 2167−2184.

(6) Cohen, S. M. *Chem. Rev.* **2012**, *112*, 970−1000.

(7) Mercs, L.; Albrecht, M. *Chem. Soc. Rev.* **2010**, *39*, 1903−1912.

(8) Zhukhovitskiy, A. V.; MacLeod, M. J.; Johnson, J. A. *Chem. Rev.* **2015**, *115*, 11503−11532.

(9) Engel, S.; Fritz, E.-C.; Ravoo, B. J. *Chem. Soc. Rev.* **2017**, *46*, 2057−2075.

(10) Smith, C. A.; Narouz, M. R.; Lummis, P. A.; Singh, I.; Nazemi, A.; Li, C.-H.; Crudden, C. M. *Chem. Rev.* **2019**, *119*, 4986−5056.

(11) Crudden, C. M.; Horton, J. H.; Ebralidze, I. I.; Zenkina, O. V.; McLean, A. B.; Drevniok, B.; She, Z.; Kraatz, H.-B.; Mosey, N. J.; Seki, T.; Keske, E. C.; Leake, J. D.; Rousina-Webb, A.; Wu, G. *Nat. Chem.* **2014**, *6*, 409−414.

(12) Man, R. W. Y.; Li, C.-H.; MacLean, M. W. A.; Zenkina, O. V.; Zamora, M. T.; Saunders, L. N.; Rousina-Webb, A.; Nambo, M.; Crudden, C. M. *J. Am. Chem. Soc.* **2018**, *140*, 1576−1579.

(13) Franz, M.; Chandola, S.; Koy, M.; Zielinski, R.; Aldahhak, H.; Das, M.; Freitag, M.; Gerstmann, U.; Liebig, D.; Hoffmann, A. K.; Rosin, M.; Schmidt, W. G.; Hogan, C.; Glorius, F.; Esser, N.; Dähne, M. *Nat. Chem.* **2021**, *13*, 828−835.

(14) Krzykawska, A.; Wróbel, M.; Kozieł, K.; Cyganik, P. *ACS Nano* **2020**, *14*, 6043−6057.

(15) Richter, C.; Schaepe, K.; Glorius, F.; Ravoo, B. J. *Chem. Commun.* **2014**, *50*, 3204−3207.

(16) Ferry, A.; Schaepe, K.; Tegeder, P.; Richter, C.; Chepiga, K. M.; Ravoo, B. J.; Glorius, F. *ACS Catal.* **2015**, *5*, 5414−5420.

(17) Salorinne, K.; Man, R. W. Y.; Li, C.-H.; Taki, M.; Nambo, M.; Crudden, C. M. *Angew. Chem. Int. Ed. Engl.* **2017**, *56*, 6198−6202.

(18) MacLeod, M. J.; Goodman, A. J.; Ye, H.-Z.; Nguyen, H. V.-T.; Van Voorhis, T.; Johnson, J. A. *Nat. Chem.* **2019**, *11*, 57−63.

(19) Amit, E.; Berg, I.; Gross, E. *Chemistry* **2020**, *26*, 13046−13052.

(20) Sherman, L. M.; Strausser, S. L.; Borsari, R. K.; Jenkins, D. M.; Camden, J. P. *Langmuir* **2021**, *37*, 5864−5871.

(21) Vericat, C.; Vela, M. E.; Benitez, G.; Carro, P.; Salvarezza, R. C. *Chem. Soc. Rev.* **2010**, *39*, 1805−1834.

(22) Shaver, A.; Kundu, N.; Young, B. E.; Vieira, P. A.; Sczepanski, J. T.; Arroyo-Currás, N. *Langmuir* **2021**, *37*, 5213−5221.

(23) Wang, G.; Rühling, A.; Amirjalayer, S.; Knor, M.; Ernst, J. B.; Richter, C.; Gao, H.-J.; Timmer, A.; Gao, H.-Y.; Doltsinis, N. L.; Glorius, F.; Fuchs, H. *Nat. Chem.* **2017**, 152−156.

(24) Wu, C.-Y.; Wolf, W. J.; Levartovsky, Y.; Bechtel, H. A.; Martin, M. C.; Toste, F. D.; Gross, E. *Nature* **2017**, *541*, 511−515.

(25) Hurst, E. C.; Wilson, K.; Fairlamb, I. J. S.; Chechik, V. *New J. Chem.* **2009**, *33*, 1837−1840.

(26) Lovat, G.; Doud, E. A.; Lu, D.; Kladnik, G.; Inkpen, M. S.; Steigerwald, M. L.; Cvetko, D.; Hybertsen, M. S.; Morgante, A.; Roy, X.; Venkataraman, L. *Chem. Sci.* **2019**, *10*, 930−935.

(27) Nguyen, D. T.; Freitag, M.; Gutheil, C.; Sotthewes, K.; Tyler, B. J.; Böckmann, M.; Das, M.; Schlüter, F.; Doltsinis, N. L.; Arlinghaus, H. F.; Ravoo, B. J.; Glorius, F. *Angew. Chem., Int. Ed.* **2020**, *59*, 13651−13656.

(28) Trujillo, M. J.; Strausser, S. L.; Becca, J. C.; DeJesus, J. F.; Jensen, L.; Jenkins, D. M.; Camden, J. P. *J. Phys. Chem. Lett.* **2018**, *9*, 6779−6785.

(29) Willets, K. A.; Van Duyne, R. P. *Annu. Rev. Phys. Chem.* **2007**, *58*, 267−297.

(30) MacLeod, M. J.; Johnson, J. A. *J. Am. Chem. Soc.* **2015**, *137*, 7974−7977.

(31) Abdelhamid, H. N. *Microchim. Acta* **2019**, *186*, 682.

(32) Li, Y.; Cao, X.; Zhan, L.; Xue, J.; Wang, J.; Xiong, C.; Nie, Z. *Chem. Commun.* **2018**, *54*, 10905−10908.

(33) Mrksich, M. *ACS Nano* **2008**, *2*, 7−18.

(34) Helal, K. Y.; Alamgir, A.; Berns, E. J.; Mrksich, M. *J. Am. Chem. Soc.* **2018**, *140*, 8060−8063.

(35) O'Kane, P. T.; Dudley, Q. M.; McMillan, A. K.; Jewett, M. C.; Mrksich, M. *Sci. Adv.* **2019**, *5*, No. eaaw9180.

(36) Fearn, S. An Introduction to Time-of-Flight Secondary Ion Mass Spectrometry (ToF-SIMS) and Its Application to Materials Science; *IOP Concise Physics*; Morgan and Claypool Publishers, 2015.

(37) Pomastowski, P.; Buszewski, B. *Nanomaterials (Basel)* **2019**, *9*, 260.

(38) Bounichou, M.; Alévêque, O.; Breton, T.; Dias, M.; Sanguinet, L.; Levillain, E.; Rondeau, D. *J. Mater. Chem.* **2009**, *19*, 8032−8039.

(39) Crudden, C. M.; Horton, J. H.; Narouz, M. R.; Li, Z.; Smith, C. A.; Munro, K.; Baddeley, C. J.; Larrea, C. R.; Drevniok, B.; Thanabalasingam, B.; McLean, A. B.; Zenkina, O. V.; Ebralidze, I. I.; She, Z.; Kraatz, H.-B.; Mosey, N. J.; Saunders, L. N.; Yagi, A. *Nat. Commun.* **2016**, *7*, 12654.

(40) Crespo, J.; Guari, Y.; Ibarra, A.; Larionova, J.; Lasanta, T.; Laurencin, D.; López-de-Luzuriaga, J. M.; Monge, M.; Olmos, M. E.; Richeter, S. *Dalton Trans.* **2014**, *43*, 15713−15718.

(41) Taira, T.; Yanagimoto, T.; Fouquet, T.; Sakai, K.; Sakai, H.; Imura, T. *J. Oleo Sci.* **2020**, *69*, 871−882.

(42) Baker, M. V.; Barnard, P. J.; Berners-Price, S. J.; Brayshaw, S. K.; Hickey, J. L.; Skelton, B. W.; White, A. H. *Dalton Trans.* **2006**, 3708−3715.

(43) Ray, L.; Katiyar, V.; Barman, S.; Raihan, M. J.; Nanavati, H.; Shaikh, M. M.; Ghosh, P. *J. Organomet. Chem.* **2007**, *692*, 4259−4269.

(44) DeJesus, J. F.; Sherman, L. M.; Yohannan, D. J.; Becca, J. C.; Strausser, S. L.; Karger, L. F. P.; Jensen, L.; Jenkins, D. M.; Camden, J. P. *Angew. Chem., Int. Ed.* **2020**, *59*, 7585−7590.

(45) La Spina, R.; Spampinato, V.; Gilliland, D.; Ojea-Jimenez, I.; Ceccone, G. *Biointerphases* **2017**, *12*, No. 031003.

(46) Chiang, C.-K.; Chen, W.-T.; Chang, H.-T. *Chem. Soc. Rev.* **2011**, *40*, 1269−1281.

(47) Harkness, K. M.; Balinski, A.; McLean, J. A.; Cliffel, D. E. *Angew. Chem. Int. Ed. Engl.* **2011**, *50*, 10554−10559.

(48) Pluchinsky, A. J.; Wackelin, D. J.; Huang, X.; Arnold, F. H.; Mrksich, M. *J. Am. Chem. Soc.* **2020**, *142*, 19804−19808.

(49) Bakker, A.; Freitag, M.; Kolodzeiski, E.; Bellotti, P.; Timmer, A.; Ren, J.; Schulze Lammers, B.; Moock, D.; Roesky, H. W.; Mönig, H.; Amirjalayer, S.; Fuchs, H.; Glorius, F. *Angew. Chem. Int. Ed. Engl.* **2020**, *59*, 13643−13646.

(50) Du, L.; Nosratabad, N. A.; Jin, Z.; Zhang, C.; Wang, S.; Chen, B.; Mattoussi, H. *J. Am. Chem. Soc.* **2021**, *143*, 1873−1884.

(51) Müller, W. H.; Verdin, A.; De Pauw, E.; Malherbe, C.; Eppe, G. *Mass Spectrom. Rev.* **2020**, 1−48.

https://doi.org/10.1021/acs.analchem.1c02401
Anal. Chem. 2021, 93, 13534−13538